The Unexpected and Large Enhancement of the Dipole Moment in the 3,4-Bis(dimethylamino)-3-cyclobutene-1,2-dione (DMACB) Molecule upon Crystallization: A New Role of the Intermolecular CH···O Interactions

Emanuela May,[†] Riccardo Destro,[†] and Carlo Gatti*[,‡]

Contribution from the Dipartimento di Chimica Fisica ed Elettrochimica, Università degli Studi di Milano, via C. Golgi 19, 20133 Milano, Italy, and Centro CNR per lo Studio delle Relazioni tra Struttura e Reattività Chimica, via C. Golgi 19, 20133 Milano, Italy

Received February 5, 2001

Abstract: The molecular dipole moment of the 3,4-bis(dimethylamino)-3-cyclobutene-1,2-dione (DMACB) molecule and its enhancement in the crystal was evaluated by periodic RHF ab initio computations. A discrete boundary partitioning of the electronic density that allows an unambiguous partitioning of the molecular space in the condensed phase was adopted. The resulting molecular dipole in the crystal compares favorably with the experimental value obtained by a multipolar analysis of single-crystal X-ray diffraction data recorded at 20 K, using a fuzzy boundary partitioning of the derived pseudoatom densities. We show that a large and highly significant molecular dipole enhancement may occur upon crystallization, despite the lack of a strongly hydrogen bonded environment in the crystal. The 23 unique C−H···O interactions which are formed upon packing of the DMACB molecule induce an increase in the molecular dipole (over 75%) that is comparable to or greater than that found in systems which are characterized by the stronger O−H···O and N−H···O hydrogen bonds. The DMACB molecule constitutes an excellent system for the study of C−H···O interactions in the condensed phase, since no other kind of competing hydrogen bonds is present in its crystal. A simple and qualitative model for the matrix contribution to the DMACB molecular dipole enhancement in the crystal is proposed. The formation of several weak C−H···O bonds is found to yield a small (about 0.2 e) net flux of electronic charge flowing from the hydrogens of the methyl groups to the carbonyl oxygen atoms. Despite the limited increase of the intramolecular charge transfer upon crystallization, a large molecular dipole enhancement occurs because the centroids of the positive and negative induced charges are quite far apart. This work highlights a new and important role of the C−H···O bond, besides those already known in the literature.

Introduction

Although it has long been known that C−H groups may form weak hydrogen bonds, the characteristics of these interactions are only recently being systematically explored.[1−5] These weak bonds frequently occur in important biological systems as carbohydrates,[6,7] nucleosides,[5] and proteins.[8,9] Their importance in crystal engineering has been recognized,[4,10] since CH···O contacts may have a determining effect on packing motifs.[11−13] In many instances these bonds also play significant roles in molecular conformation,[14−17] in molecular recognition processes,[18,19] and in the stability of biological macromolecules.[8,20]

As recently pointed out by Steiner,[2] most of the studies of CH···O hydrogen bonds have so far concentrated on their role, rather than on their specific nature. In a companion paper,[21] we have shown the wealth of information one obtains—from an analysis of experimental and theoretical crystalline electron densities ρ—on the nature of these weak interactions in the condensed phase. The system we investigated was the crystal of the 3,4-bis(dimethylamino)-3-cyclobutene-1,2-dione molecule

* Address correspondence to this author: (e-mail) c.gatti@csrsrc.mi.cnr.it.
[†] Università degli Studi di Milano.
[‡] Centro CNR per lo Studio delle Relazioni tra Struttura e Reattività Chimica.

(1) Steiner, T. *Cryst. Rev.* **1996**, *6*, 1.
(2) Steiner, T. *Chem. Commun.* **1997**, 727 and references therein.
(3) Jeffrey, G. A. *An Introduction to Hydrogen Bonding*; Oxford University Press: Oxford, UK, 1997.
(4) Desiraju, G. R. *Acc. Chem. Res.* **1991**, *24*, 290.
(5) Jeffrey, G. A.; Saenger, W. *Hydrogen Bonding in Biological Structures*; Springer: Berlin, 1991.
(6) Steiner, T.; Saenger, W. *J. Am. Chem. Soc.* **1992**, *114*, 10146.
(7) Steiner, T.; Saenger, W. *J. Am. Chem. Soc.* **1993**, *115*, 4540.
(8) Derewenda, Z. S.; Lee, L.; Derewenda, U. *J. Mol. Biol.* **1995**, *252*, 248.
(9) Musah, R. A.; Jensen, G. M.; Rosenfield, R. J.; McRee, D. E.; Goodin, D. B.; Bunte, S. W. *J. Am. Chem. Soc.* **1997**, *119*, 9083.
(10) Braga, D.; Angeloni A.; Grepioni, F.; Tagliavini, E. *Chem. Commun.* **1997**, 1447.
(11) Berkovitch-Yellin, Z.; Leiserowitz, L. *Acta Crystallogr.* **1984**, *B40*, 159.
(12) Desiraju, G.; Kashino, S.; Coombs, M. M.; Glusker, J. *Acta Crystallogr.* **1993**, *B49*, 880.
(13) Sarma, J.A. R. P.; Desiraju, G. R. *Acc. Chem. Res.* **1986**, *19*, 222.
(14) Seiler, P.; Dunitz, J. D. *Helv. Chim. Acta* **1989**, *72*, 1125.
(15) Chao, I.; Chen. J.-C. *Angew. Chem.* **1996**, *108*, 200.
(16) Müller, G.; Lutz, M.; Harder, S. *Acta Crystallogr.* **1996**, *B52*, 1014.
(17) Saenger, W.; Steiner, T. *Acta Crystallogr.* **1998**, *A54*, 798.
(18) Shimon, L. J. W.; Vaida, M.; Addadi, L.; Lahav, M.; Leiserowitz, L. *J. Am. Chem. Soc.* **1990**, *112*, 6215.
(19) Desiraju, G. R. *Angew. Chem., Int. Ed. Engl.* **1995**, *34*, 2311.
(20) Leonard, G. A.; McAuley-Hecht, K.; Brown, T.; Hunter, W. N. *Acta Crystallogr.* **1995**, *D51*, 136.
(21) Gatti, C.; May, E.; Destro, R.; Cargnoni, F. *J. Phys. Chem.* Submitted for publication.

10.1021/ja010316m CCC: $20.00
Published on Web 11/13/2001

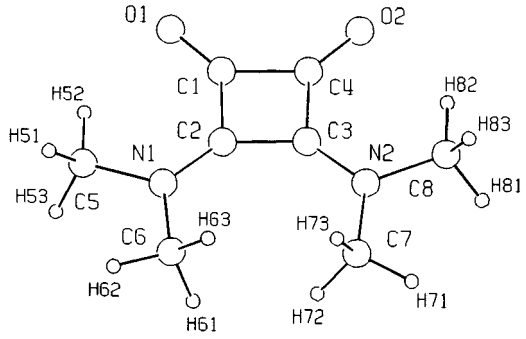

Figure 1. Atomic labels for the DMACB molecule. When reporting their labels throughout the text, the corresponding atoms of the two independent A and B molecules in the crystal are differentiated by appending an "A" or a "B", respectively, to the atomic labels shown in this figure.

(hereinafter DMACB molecule, Figure 1). In the present paper we report a study on this same system but highlighting a potential role (in Steiner's terms a *function*)[2] of intermolecular CH···O interactions that, to the best of our knowledge, has never been investigated so far. The effect is the capability of intermolecular CH···O interactions to cause a very pronounced enhancement of the molecular dipole upon crystallization. This increase has never been reported for the case of the weak hydrogen bonds, while it has been well documented, both experimentally[22−26] and theoretically,[24,26−30] for molecules in strongly hydrogen bonded environments. Its occurrence was found in these latter cases to be generally due to some charge transfer from hydrogens to their acceptor atoms (e.g. water, urea, imidazole, cytosine, formamide, and acetamide). The aim of this paper is to explore whether also the weak CH···O bonds can induce a significant intramolecular charge transfer and, consequently, a large molecular dipole enhancement upon crystallization. It is worth noting that the DMACB crystal represents a particularly well suited system for analyzing this potential effect of the C−H···O interactions, since no other kind of competing and stronger hydrogen bond is present in the crystal.

A recent room-temperature X-ray diffraction study[31] showed that in the solid the DMACB molecule adopts a nearly coplanar conformation for all non-H atoms, whereas in the gas phase, ab initio computations assign a C_2 minimum energy conformation to the DMACB molecule, with $C_{ring}-C_{ring}-N-C_{methyl}$ torsion angles of about 40°.[32]

An obvious explanation for the difference in conformation is the influence of the intermolecular interactions acting in the crystal, where strong dipole−dipole interactions and a large number of CH···O contacts are observed.[33] The adoption of a planar conformation in the solid allows enhancement of the energetic weight of the dipole−dipole interactions arising from the head-to-tail arrangement of the molecular dipole moments along each column of the crystal.[31] Conversely, the CH···O contacts not only represent a significant energetic contribution to the crystalline interaction energy on their own,[21] but they might also have a possibly more important, yet indirect, energy effect if they cause a significant molecular dipole moment increase upon crystallization. The DMACB molecule has, in its C_2 symmetry gas-phase conformation, a large dipole moment, of about 7 D, directed along the rotation axis; an increase of this dipole in the bulk, provided the molecules arrange in favorable mutual orientations in the crystal, would automatically increase the energetic contribution to the crystal packing energy of the charge−dipole and dipole−dipole interactions. This induced dipole, if any, would then add up to the variation in dipole caused by the geometrical change occurring in the bulk.

The analysis presented in this paper discloses the mechanisms and relative weights of the geometry change and of the crystal field effects in determining the induced dipole moment in the crystal, using a theory[34] that allows an unambiguous partitioning of the molecular and atomic charge density in a condensed phase also.[27,28,35]

Experimental and Computational Details

The experimental electron density of the $P\bar{1}$ phase of the DMACB crystal was derived from a low-temperature (20 K) X-ray diffraction study.[36] Details of data collection and multipole refinements will be published elsewhere.[37] Figure 2a shows columns of stacked DMACB molecules extending parallel to the crystallographic axis *a*, while Figure 2b illustrates how the N−C−C−N fragment of one molecule, when viewed down the axis of the stack, lies just above and below the O−C−C−O fragment of neighboring molecules within each column. Molecules of different columns are related by the 2_1 axis in the room-temperature monoclinic phase; below 147 K a second-order phase transition to the triclinic $P\bar{1}$ space group occurs, and the 2_1 symmetry is lost. Since this structural modification induced by the phase transformation is rather modest, at 20 K the two molecules in the asymmetric unit (A and B, Figure 2a,b) are still very similar to one another. Figure 3a,b shows respectively the *inter*- and the *intra*-column C−H···O bonds which are found for H···O contacts below 3 Å, according to the charge density topology.[21]

The electron density was described by a finite multipolar expansion of atom-centered functions, according to the "pseudo-atom" formalism due to Stewart,[38] and the VALRAY[39] set of programs was employed for the refinements. The adopted models included multipoles up to octupole terms on heavy atoms, and up to quadrupole terms on hydrogen atoms. The H atoms were treated as anisotropic and their anisotropic displacement parameters—held fixed in the refinement—were determined independently by combining information from TLS thermal motion analysis of non-H atoms and from infrared vibrational frequencies, using the ADPH code.[40] Refinement of 817 variables, using 12674 observations within $(\sin\theta/\lambda)^{Max}_{Mo} = 1.14$ Å^{-1}, gave a final agreement index, R_F, and a goodness-of-fit equal to 0.0253 and 1.051, respectively.

(22) Spackman, M. A. *Chem. Rev.* **1992**, *92*, 1769 and references therein.
(23) Howard, S. T.; Hursthouse, M. B.; Lehmann, C. W.; Mallinson, P. R.; Frampton, C. S. *J. Chem. Phys.* **1992**, *97*, 5616.
(24) Abramov, Yu. A.; Volkov, A. V.; Coppens, P. *Chem. Phys. Lett.* **1999**, *311*, 81.
(25) Zhang, Y.; Coppens, P. *Chem. Commun.* **1999**, 2425.
(26) Volkov, A.; Gatti, C.; Abramov, Y.; Coppens, P. *Acta Crystallogr.* **2000**, *A56*, 252.
(27) Gatti, C.; Saunders, V. R.; Roetti, C. *J. Chem. Phys.* **1994**, *101*, 10686.
(28) Gatti, C.; Silvi, B.; Colonna, F. *Chem. Phys. Lett.* **1995**, *247*, 135.
(29) Spackman, M. A.; Byrom, P. G.; Alfredsson, M.; Hermansson, K. *Acta Crystallogr.* **1999**, *A55*, 30.
(30) Silvestrelli, P. G.; Parrinello, M. *Phys. Rev. Lett.* **1999**, *82*, 3308.
(31) Lunelli, B.; Roversi, P.; Ortoleva, E.; Destro, R. *J. Chem. Soc., Faraday Trans.* **1996**, *92*, 3611.
(32) The constrained (C_s) gas-phase planar conformation possesses an imaginary frequency normal mode and represents a transition state between the two degenerate C_2 minimums. The absence of a C_s stable conformation in the gas phase is likely to be the result of the destabilizing effect of the four short H−H contacts which characterize the C_s conformation, instead of the single short contact present in the C_2 form.[31]
(33) Conformational changes due to matrix effects have been previously reported. See for example: Popelier, P.; Lenstra, A. T. H.; Alsenoy, C. V.; Geise, H. J. *J. Am. Chem. Soc.* **1989**, *111*, 5658.
(34) Bader, R. F. W. *Atoms in Molecules: A Quantum theory*; Int. Ser. Monogr. Chem., No. 22; Oxford University: Oxford, 1990.
(35) Zou, P. F.; Bader, R. F. W. *Acta Crystallogr.* **1994**, *A50*, 714.
(36) Crystal data for the $P\bar{1}$(19K) phase: $C_8H_{12}N_2O_2$, $Z = 4$, $a = 6.7965(6)$ Å, $b = 13.7743(15)$ Å, $c = 8.7727(16)$ Å; $\alpha = 90.05(1)°$, $\beta = 101.89(1)°$, $\gamma = 91.96(2)°$. See: Destro, R. *Chem. Phys. Lett.* **1997**, *275*, 463.
(37) Destro, R.; May, E.; Gatti, C. To be submitted for publication.
(38) Stewart, R. F. *Acta Crystallogr.* **1976**, *A32*, 565.
(39) Stewart, R. F.; Spackman, M. A. *VALRAY User's Manual*; Department of Chemistry, Carnegie-Mellon University, Pittsburgh, 1983.
(40) Roversi, P. MSc thesis, Milano, 1992.

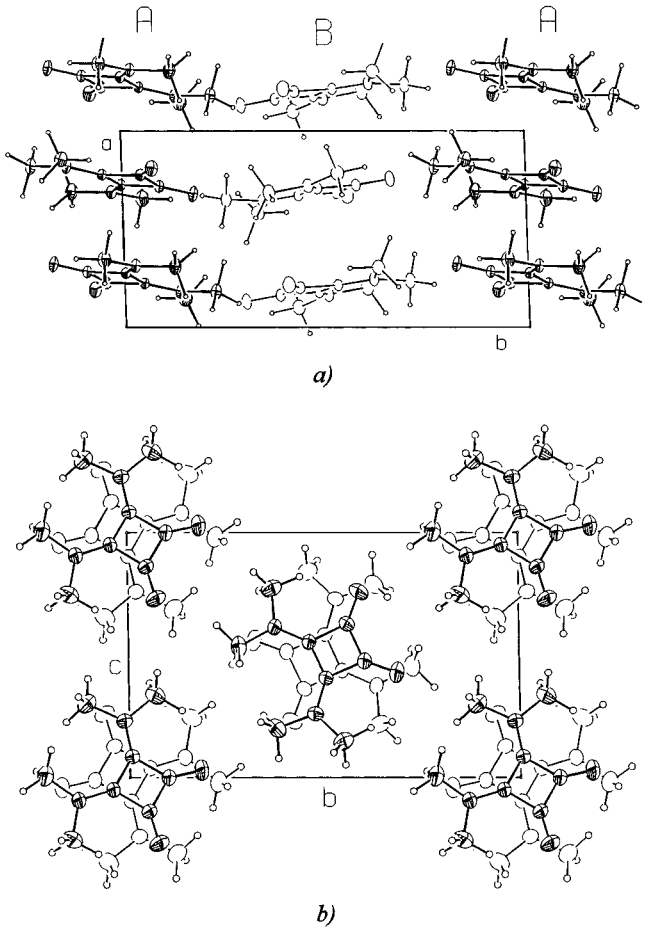

Figure 2. Crystal packing ($P\bar{1}$ phase) of DMACB molecules (a) viewed along the *c* and (b) *a* axes. A and B denote the two (different) DMACB molecules in the unit cell.

The final average C−H distance was 1.074 Å, in very close agreement with that determined from neutron diffraction for methyl groups.[41]

Ab initio computations: Crystal wave function calculations were performed by using the Hartree−Fock−Roothaan fully periodic approach (hereinafter called PHF), as implemented in the CRYSTAL-98 code.[42] Wave functions for the A, B molecules and for an AA′ adduct were also computed so as to evaluate the molecular dipole moment enhancement on going from the molecule in the gas phase to the molecule in a crystal dimeric fragment and, finally, to the molecule in the crystal (see infra). The adduct (from now on a AA′ dimer) was formed by the closest AA′ center-symmetrically related pair in the crystal. The geometry derived from the low-temperature X-ray experiment was used for both gas-phase and crystal computations. Standard molecular local basis sets (6-21G, 6-31G*)[43] were adopted; yet, convergence problems met with the PHF/6-31G* calculations and, more importantly, the large size of our system precluded the use of the more flexible 6-31G* basis in the computation of the atomic properties in the crystal.[21] While the 6-21G estimates for the molecular dipoles in the gas or crystal phase are not expected to be particularly accurate on an absolute scale, the evaluation of the corresponding molecular dipole change—the induced dipole $\Delta\mu$—should be much more reliable. Computations on urea crystal and molecule confirm these findings.[44]

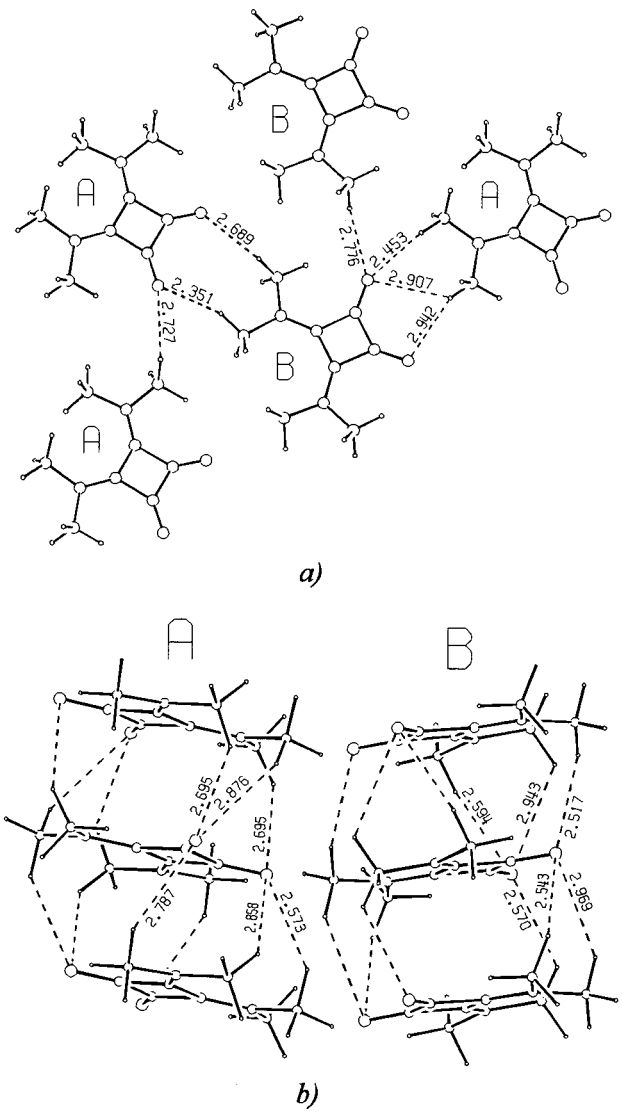

Figure 3. CH···O intermolecular interactions in DMACB crystals ($P\bar{1}$ phase) with the H···O distance below 3.0 Å. Only the bonded interactions, as determined by the charge density topology, are shown.[21] The oxygen atoms are involved in up to 6 intermolecular hydrogen bonds. (a) Intercolumn interactions: the oxygen atoms of an A (or B) molecule form a total of 2 (or 3) H-bonds with the methyl groups of a B (or A) molecule in neighboring columns, and one bond with a molecule of the same type A (or B), related by translation along the *c* axis. Intracolumn interactions: the oxygen atoms of either molecule A or B in a column form a total of 6 intermolecular H-bonds, 3 with the H atoms of the molecule above and 3 with those of the molecule below. Each center-symmetric AA′ or BB′ pair is thus linked by 6 CH···O interactions.

The relaxation of the DMACB crystal geometry in the gas phase has been previously investigated,[31] using computational approaches of increasing quality (up to the MP2/6-31G* level) and within the C_2 symmetry constraint. For the sake of comparison with crystal calculation, a geometry optimization of the DMACB molecule, at the 6-21G level, was also performed. Systems at crystal or at gas-phase optimized geometry are referred to in the following as CG or OG systems, respectively.

Atomic properties: The Quantum Theory of Atoms in Molecules (QTAM)[34] enables one to define an atom in a molecule or in a crystal as a finite nonoverlapping entity in real space.[35] The atom, Ω, is the

(41) Allen, F. H.; Kennard, O.; Watson, D. G.; Brammer, L.; Orpen, A. G.; Taylor, R. In *International Tables for crystallography*; Wilson, A. J. C., Ed.; Kluwer Academic Publishers: Dordrecht, The Netherlands, 1995; Vol. C, pp 696.

(42) Saunders: V. R.; Dovesi, R.; Roetti, C.; Causà, M.; Harrison, N. M.; Orlando, R.; Zicovich-Wilson, C. M. *CRYSTAL98, User's Manual*; University of Torino: Torino, 1998.

(43) Hehre, W. J.; Radom, L.; Schleyer, P. v. R.; Pople, J. A. *Ab Initio Molecular Orbital Theory*; Wiley-Interscience: New York, 1986, and references therein.

(44) $|\Delta\boldsymbol{\mu}|$ for urea is 1.9(2.4) D at the PHF/6-31G** and 2.2(2.5) D at the PHF/6-21G level using crystal (gas-phase optimized) geometries in the molecular calculation. 6-31G** data from ref 27, while 6-21G results are unpublished (C. Gatti).

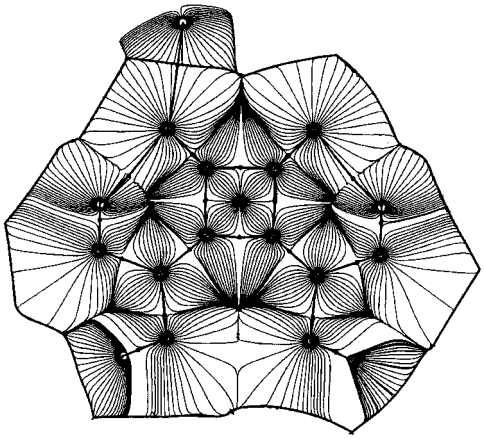

Figure 4. The DMACB molecule in the crystal as defined by the $\nabla\rho$ trajectories. The bond paths[34] related to intra- or intermolecular bonds and the intersections of the molecular zero-flux surface with the molecular plane are marked by heavy lines. Bond critical points[34] are denoted by dots.

union of a nucleus at $\mathbf{r}_\Omega$ and its associated basin, defined as the portion of space including the nucleus and bounded by a surface S of local zero flux in the gradient vector of the electron density, $\rho(\mathbf{r})$. Integration of the electron density over the basin of atom Ω gives its atomic population N_Ω, while the average of the vector $-(\mathbf{r} - \mathbf{r}_\Omega)$ over the electron density in the same basin, gives the first moment $\boldsymbol{\mu}_\Omega$ of an atom's electron distribution. The first moments, or atomic dipoles $\boldsymbol{\mu}_\Omega$, arise from polarization of the atomic electron densities.

QTAM atomic populations and first moments were only computed for theoretical densities, using PROMEGA[45] and PROAIMV[46] programs in the case of nonperiodic systems and TOPOND98[47] code for atoms in the crystal. The total number of integrated electrons differed from the theoretical value by less than 0.009 au in all the investigated systems.[21]

In-crystal dipole moments: The determination of molecular dipole moment from the total (nuclear plus electron) density within a crystal requires defining (i) a molecule in a crystal and (ii) the charge density associated with the molecule. While there is no problem in recognizing a molecular fragment in a case such as the DMACB crystal, the space partitioning of a continuous charge distribution—as is the electronic component of the total density—may be accomplished according to several schemes.[22,48] These fall in two main classes, one characterized by a *discrete boundary* partitioning, with the density at each point being assigned to a specific atomic or molecular basin, and a second distinguished by a *fuzzy boundary* partitioning, with the density at each point being apportioned among overlapping functions centered at different locations. These two alternative boundaries lead to nonoverlapping and to interpenetrating molecular fragments, respectively.

Space division according to QTAM is an example of discrete boundary partitioning and is here applied to the evaluation of molecular dipole moment from the theoretical crystalline electron density. Figure 4 displays how a DMACB molecular entity is identified within the DMACB crystal by using the $\nabla\rho$ vector field and the zero-flux boundary condition. Such a method has the serious drawback of being much more computationally demanding than other discrete boundary approaches,[49−53] but it has the great advantage of being the only approach that isolates a *proper* molecular fragment, one to which all of the theorems of quantum mechanics apply.[34,54,55]

The molecular dipole $\boldsymbol{\mu}$ in the crystal and in the isolated molecules has been decomposed[27,28,55] into a first moment contribution $\boldsymbol{\mu}_A$ given by the sum of the atomic first moments ($\boldsymbol{\mu}_A = \sum_\Omega \boldsymbol{\mu}_\Omega$) and a charge-transfer contribution $\boldsymbol{\mu}_{CT}$ ($\boldsymbol{\mu}_{CT} = \sum_\Omega q_\Omega \mathbf{r}_\Omega$) arising from the net atomic charges q_Ω ($q_\Omega = Z_\Omega - N_\Omega$; Z_Ω being the nuclear charge of Ω).[56]

In the case of the experimental densities a different partitioning scheme was adopted. The atom-centered multipolar expansion used in the least-squares refinement of X-ray intensities yields by its nature a fuzzy boundary division of crystalline electron density. Within VALRAY formalism, the electron density of a molecular moiety removed from the lattice—and nonetheless reflecting the interaction with the crystal environment—is given by the sum of the continuous densities of its constituting pseudo-atoms. Once the multipole refinement is completed, the determination of the molecular moiety dipole moment is straightforward.[57] Analogously to the decomposition afforded within the QTAM framework, the molecular dipole may be expressed as a sum of first moment atomic contributions, deriving from the coefficients of the dipole deformation functions, and of charge-transfer terms, arising from monopole net populations.[58] To avoid any residual origin dependence,[59] the monopole population parameters were re-scaled as to yield a perfectly neutral molecule. Such re-normalization was deemed possible since no detectable[60] charge transfer was found to occur between the two molecules in the DMACB crystal, according to both experiment and theory.

A QTAM partitioning was not performed for the DMACB experimental density because the only VALRAY version available[39] when this work was in preparation did not include such an option. Very recently, an updated version[61,62] of VALRAY code and an interface, named TOPXD,[26,63] of TOPOND-98 to the multipolar XD package[64] have appeared. Both these codes include the evaluation of QTAM atomic properties. Yet, it has been shown that, contrary to the values of the individual atomic charges of the atoms constituting the molecule, the molecular dipole moment in the crystal is only marginally affected by the partitioning scheme (either QTAM or multipole-model based) adopted for the experimental densities.[26,62] This is a gratifying result in consideration of some conceptual approximations we unavoidably introduced when using either schemes to evaluate the molecular dipole in the crystal. Indeed, in the case of the multipole-based partitioning,

(45) Keith, T. A. Ph.D. Thesis, McMaster University, 1993.
(46) PROAIMV, McMaster University, Ontario, Canada, 1992.
(47) Gatti, C. *TOPOND-98: an electron density topological program for systems periodic in N (N=0−3) dimensions*; User's Manual, CNR-CSRSRC, Milano, 1999.
(48) Coppens, P. *X-ray Charge Densities and Chemical Bonding*; IUCr Texts on Crystallography, No. 4: Oxford Science Publications: Oxford, 1997.
(49) Wigner, E.; Seitz, F. *Phys. Rev.* **1933**, *43*, 804.
(50) Coppens, P. *Phys. Rev. Lett.* **1975**, *35*, 98.
(51) Moss, G.; Coppens, P. *Chem. Phys. Lett.* **1980**, *75*, 298.
(52) Spackman, M. A.; Byrom, P. G. **1997**, *267*, 215.
(53) Mitchell, A. S.; Spackman, M. A. **2000**, *21*, 933.
(54) Bader, R. F. W. *Phys. Rev.* **1994**, *B49*, 13348.
(55) Bader, R. F. W.; Larouche, A.; Gatti, C.; Carroll, M. T.; MacDougall, P. J.; Wiberg, K. B. *J. Chem. Phys.* **1987**, *87*, 1142.
(56) In the case of the isolated systems, where molecular boundaries are at infinite, the precision of the obtained dipole moments could be estimated by comparing them with those evaluated through the standard theoretical procedure [$\boldsymbol{\mu} = \sum_\Omega Z_\Omega \mathbf{r}_\Omega - tr(P\mathbf{D})$, P and $\mathbf{D}$ being the density and the dipole matrices on atomic basis, respectively]. Differences were in any case less than 0.05 D.
(57) Stewart, R. F. *J. Chem. Phys.* **1972**, *57*, 1664.
(58) Two main disadvantages are known (refs 48 and 24) for dipole moment determination based on multipole partitioning. The first is that any density not fitted by the model is discarded in the partitioning process. The second is that very diffuse functions of the model, if included, violate the requirement of locality—that is that the density at a point should be assigned to a center in the proximity of that point. Such a violation may lead to biased and counterintuitive results (refs 24 and 48). These drawbacks were not deemed important in our case since (i) the residual density does not exceed 0.02 e/Å^3 at any point and (ii) the radial functions of the deformation poles are not particularly diffuse as their exponents were fixed at the standard molecular values (Hehre, W. J.; Stewart, R. F.; Pople, J. A. *J. Chem. Phys.* **1969**, *51*, 2657).
(59) Coppens, P.; Volkov, A.; Abramov, Y.; Koritsanszky, T. *Acta Crystallogr.* **1999**, *A55*, 965.
(60) The computed standard deviation (0.15) of the sum of monopole populations was greater than the deviation from electron-neutrality for both molecules A ad B.
(61) Stewart, R. F.; Spackman, M. A.; Flensburg, C. *Valray-98 User's Manual*, version 2.1, July 2000; Carnegie Mellon University and University of Copenhagen.
(62) Flensburg, C.; Madsen, D. *Acta Crystallogr.* **2000**, *A56*, 24.
(63) Volkov, A.; Gatti, C. *TOPXD User's Manual*, version 2.0, December 2000, SUNY−Buffalo (USA) and CNR-CSRSRC, Milano (Italy).
(64) Koritsanszky, T.; Howard, S.; Su, Z.; Mallinson, P. R.; Richter, T.; Hansen, N. K. *XD—A Computer Program Package for Multipole Refinement and Analysis of Electron Densities from Diffraction Data*; Free University of Berlin: Berlin, Germany, 1997.

Table 1. Effect of Geometry, Gas-Phase Molecular Association, and Crystal Packing on the DMACB Molecular Dipole Moment (D)[a]

system		RHF/6-21G	RHF/6-31G*	exptl
OG molecule[b]		7.30	6.86	
CG molecule[b]	A	8.41	9.07	
	B	8.41	9.10	
dimer	AA′	9.85	11.48	
crystal	A	12.99[c]		16.6(13)
	B	12.61[c]		16.2(12)

[a] 1 D = 2.54176 au. [b] OG: gas-phase optimized geometry. CG: crystal geometry. [c] PHF/6-21G density.

the boundaries of the molecule in the crystal have been tacitly assumed to be at the infinite, while they are not obviously so in reality.[65] On the other hand, using QTAM boundaries, one should have also included the contribution to the polarization arising from the surface transfer charges between the molecules.[66] Such a contribution should not in general vanish even when, as in our case, any kind of intermolecular charge transfer does take place.[67] However, it should be small in value for a neutral molecule and negligibly small compared to the induced dipole moment, if any.[68,69]

Results and Discussion

In-crystal dipole moment: diffraction and theoretical results for the dipole moment of molecules A and B in the crystal are given in Table 1.[70] Theoretical data for isolated molecules and AA′ dimer are also there reported. Packing forces strongly increase the DMACB molecular dipole; a thorough analysis of such an enhancement is delayed to the next paragraphs, after a comparison of the experimental and theoretical dipole estimates for the bulk.

Theory (6-21G basis) predicts crystalline molecular dipoles for the A and B molecules which are about 20% smaller than the corresponding experimental estimates. However, these differences in the dipole moment predictions are only about twice the experimental esd's for both A and B molecules. This substantial agreement[71] could even significantly improve if one could also exploit the PHF/6-31G* level of theory, as one may infer from the trend of RHF/6-31G* dipole values on passing from OG to CG molecules and then to the AA′ dimer.

As expected from their geometrical similarity, A and B molecules exhibit molecular dipole moments in the crystal which differ, experimentally, by a nonsignificant amount with respect to their esd's and, computationally, by less than 0.4 D. Yet, both experiment and theory predict a slightly greater dipole moment for the A molecule. Since A and B molecules have equal gas-phase dipole moment (RHF results), the small difference found in the bulk indicates that these molecules experience slightly dissimilar intermolecular interactions in the crystal.[21]

Table 2. First Moment ($\boldsymbol{\mu}_A$) and Charge Transfer ($\boldsymbol{\mu}_{CT}$) Contributions to the RHF (or PHF, bulk) 6-21G DMACB Molecular Dipole Moment $\boldsymbol{\mu}$ (Values in D)

contribution	OG molecule	CG molecule A[a]	dimer AA′	bulk A	bulk B
$\boldsymbol{\mu}_A$[b]	2.64	2.14	2.23	2.18	2.21
$\boldsymbol{\mu}_{CT}$[b]	9.89	10.49	12.03	15.17	14.81
$\boldsymbol{\mu} = (\boldsymbol{\mu}_A + \boldsymbol{\mu}_{CT})$	7.25	8.36	9.85	12.99	12.61

[a] The A and B molecules have equal dipole moment in the gas phase (RHF/6-21G results). [b] The components parallel to $\boldsymbol{\mu}$ are reported. The projected values amount to over 99.9% of the corresponding contribution magnitudes.

Induced dipole moment—the effect of geometry change: Table 2 shows that theory predicts a dipole moment enhancement that amounts to 5.69 or 5.31 D, on passing from the OG molecule in the gas phase to the A or B molecules in the crystal, respectively. These induced dipoles represent about 78 and 72% of the gas-phase molecular dipole and are due to the influence of the crystal environment on the molecular geometry and charge distribution. Comparison of CG and OG molecular dipoles shows that the geometry change accounts for some 20% of the total induced dipole moment, while the electron density polarization caused by the matrix yields the remaining 80%. The polarization induced by the closest A′ neighbor on a A molecule constitutes over 32% of such a matrix effect.

Table 2 details the first moment, $\boldsymbol{\mu}_A$, and the charge transfer, $\boldsymbol{\mu}_{CT}$, contributions to the DMACB molecular dipoles in the monomers, the AA′ dimer, and the crystal. Because of the fields created by the charge transfer (CT), the atomic charge distributions become polarized in a direction opposite to that of CT. Therefore, in our systems the μ_A always opposes the μ_{CT} term (μ_A and μ_{CT} being the projected components of $\boldsymbol{\mu}_A$ and $\boldsymbol{\mu}_{CT}$ along $\boldsymbol{\mu}$). As the dominant contribution to the dipole is given by the CT term (Table 2), the total dipole has the same direction of $\boldsymbol{\mu}_{CT}$ and it is only somewhat smaller in magnitude.

On passing from the OG to the CG molecule, the dipole magnitude raises as a result of a $\boldsymbol{\mu}_{CT}$ increase and a similar $\boldsymbol{\mu}_A$ decrease. A qualitative account of this geometry-induced[72] $\boldsymbol{\mu}_{CT}$ enhancement is here given in terms of a *bond dipole* model, of the kind used by Bader et al.[55] for interpreting the vibrationally induced molecular dipoles in ethylene. The bond dipole of the two out-of-plane $N-C_{methyl}$ bonds in the C_2 6-21G molecule amounts to 3.07 D. Each one of these bond dipoles is composed of an in-plane component directed along the C_2 axis and contributing to the total molecular dipole and of an out-of-plane component that is canceled by the corresponding component of the other out-of-plane $N-C_{methyl}$ bond. If the two out-of-plane $N-C_{methyl}$ bonds of the OG molecule are forced to lie in the plane of the four-membered ring (4MR), while not allowing any interatomic charge transfer, the contribution from these two C−N bond dipoles to the induced $\boldsymbol{\mu}_{CT}$ is simply given by twice the difference between the magnitude and the projection on the

(65) In other words, though the DMACB electron density reflects the interaction of the molecule with the crystal environment, the molecular boundaries have been artificially moved to infinity, and thus with no allowance of electronic charge on them.

(66) Bader, R. F. W.; Matta, C. F. *Int. J. Quantum Chem.*, **2001**, *85*, 592.

(67) The evaluation of such a contribution would require the knowledge of the integral of the electric field flux through the QTAM intermolecular surfaces in the crystal. We are currently developing a new TOPOND version that will compute these surface integrals also.

(68) Keith, T. A.; Bader, R. F. W. *J. Chem. Phys.* **1992**, *96*, 3447.

(69) In the case of molecular adducts, it is possible to re-express the charge-transfer contribution to the total dipole moment as a sum of intramolecular and intermolecular charge-transfer terms (ref 68). However, it has been shown in the case of NH_3-SiF_4 adduct that even in the presence of a large intermolecular charge transfer ($q_{NH_3} = 0.082$) the contribution to the induced dipole moment arising from the surface transfer charges is less than 20% [ref 68].

(70) It has been recently shown (ref 26) that the induced dipole moments in crystals—determined through a multipole refinement of computed (PHF) static structure factors—are very close to those obtained directly from the PHF electron density. These results make us quite confident that the multipole treatment of intensity data should not seriously bias the significance of the comparison presented in Table 1.

(71) Experiment and theory also show the same μ orientation since its z component—directed through the midpoints of C1−C4 and C2−C3 bonds—turns out to be more than 99% of the total dipole magnitude for A and B molecules and with both approaches.

(72) The most noticeable changes from OG to CG molecule concern the loss of pyramidalization at the N atoms and the concomitant decrease of the $C_{ring}-C_{ring}-N-C_{methyl}$ torsion angles from about 26° down to a maximum of 6° (*B* molecule) in the crystal (RHF/6-21G results).

Table 3. Atomic Electron Population Changes $\Delta N\Omega$ (Bulk − CG Molecule) upon Crystallization[a)]

molecule A Ω	$\Delta N\Omega$	molecule B Ω	$\Delta N\Omega$
O1A	0.087	O1B	0.084
O2A	0.087	O2B	0.082
N1A	0.005	N1B	0.004
N2A	0.011	N2B	0.013
C1A	0.005	C1B	0.014
C2A	−0.034	C2B	−0.029
C3A	−0.033	C3B	−0.028
C4A	0.005	C4B	0.010
C5A	0.003	C5B	0.021
C6A	0.045	C6B	0.047
C7A	0.010	C7B	0.002
C8A	0.008	C8B	0.013
H51A	−0.025	H51B	−0.035
H52A	0.033	H52B	0.036
H53A	−0.024	H53B	−0.037
H61A	−0.035	H61B	−0.027
H62A	−0.052	H62B	−0.067
H63A	−0.006	H63B	−0.002
H71A	−0.004	H71B	−0.013
H72A	−0.021	H72B	−0.023
H73A	−0.046	H73B	−0.028
H81A	−0.022	H81B	−0.038
H82A	0.036	H82B	0.025
H83A	−0.035	H83B	−0.020

[a] Refer to Figure 1 and its caption for atomic labeling.

4MR of one of them. That is, $|\Delta\boldsymbol{\mu}| = 2 \times 3.07[1 - \cos(26°)] = 0.62$ D, a value that compares favorably with the computed $\Delta\boldsymbol{\mu}_{CT}$(OG→ CG) value (0.60 D, Table 2). The merit of this analysis is to isolate a simple and spatially localized cause for the observed $\Delta\boldsymbol{\mu}_{CT}$. Changes in the $\boldsymbol{\mu}_A$ contributions are less localized and not easily amenable to a simple model explanation.

The combined effect of the dipole moment enhancement and of the much closer packing allowed by the planar arrangement may explain the occurrence of the CG conformer in the crystal. It appears that the associated energy stabilization outweighs the destabilizing effect due to the four short H−H contacts present in the CG conformation, instead of the single contact existing in the OG conformer.[31]

Induced dipole moment—the effect of the electron density polarization: As stated earlier, the electron density polarization due to insertion of the DMACB molecule in the crystal yields the remaining 80% of the total induced dipole. Table 2 shows that the atomic polarization accounts for only 2% of this quantity,[73] the dominant contribution being due to the changes in the interatomic charge transfers, which are caused by the presence of the neighboring molecules in the bulk. These interatomic charge rearrangements are thus the main reason for the *total* induced dipole enhancement on passing from the OG molecule to the bulk. Yet, how can the weak, intra- and intercolumn C−H···O bonds induce such a large increase in the CG molecular dipole? A simple and clear-cut explanation follows. Neglecting the $\boldsymbol{\mu}_A$ variation (see the good grounds above) and considering that the geometry remains unchanged, the induced dipole $\Delta\boldsymbol{\mu}$ may be written as $\Delta\boldsymbol{\mu} = \boldsymbol{\mu}_{cryst} - \boldsymbol{\mu}_{molCG} \approx \sum_\Omega[-\mathbf{X}_\Omega \Delta N_\Omega]$, where $\Delta N_\Omega = N_{\Omega,cryst} - N_{\Omega,molCG}$. If one restricts the summation over Ω to the O and H atoms only, a $\Delta\boldsymbol{\mu}$ value of 4.32 D is obtained, to be compared with the corresponding "exact" value of 4.44 D (average value for the induced dipole of A and B molecules). One may conclude that the induced dipole is mainly due to variations in the atomic populations of the oxygen and hydrogen atoms. The use of a restricted summation in the above expression for $\Delta\boldsymbol{\mu}$ is justified by Table 3, which shows that the total electron population changes of oxygen or hydrogen atoms, following crystallization, are about 1 order of magnitude larger than those of nitrogen and carbon atoms. The formation of several weak C−H···O bonds yields a small (about 0.2 e for the A molecule) net flux of electronic charge flowing from the hydrogens of the methyl groups to the carbonyl oxygen atoms. As the centroids of positive and negative induced charges lie quite far apart (7.2 au in the model including only O and H atoms, or 4.8 au in the exact model including all atoms), a significant dipole enhancement occurs, despite the limited intramolecular charge transfer increase.

(73) Remember that in our system a $\boldsymbol{\mu}_A$ decrease yields a total dipole increase.

Table 4. Comparison of the Relative $|\Delta\boldsymbol{\mu}/\boldsymbol{\mu}_{mol\,OG}|$ and Absolute $|\Delta\boldsymbol{\mu}|$ Magnitudes of the Induced Dipole Moment in DMACB and in Other Systems Tied Together by O−H···O and N−H···O Hydrogen Bonds[a]

system	ref	$\lvert\Delta\boldsymbol{\mu}\rvert/\lvert\boldsymbol{\mu}_{mol\,OG}\rvert \times 100$	$\lvert\Delta\boldsymbol{\mu}\rvert$
DMACB	this work	75	5.5
PANB	24	150	13.8
PNA	24	66	5.3
	26	37−48	3.0−3.8
urea	27	53	2.4
	29	27	1.4
formamide	76	48	2.0
	29	28	1.3
DL-histidine	24	38	5.5
DL-proline·H_2O	24	38	3.7
imidazole	22	31	1.1
ice VIII	28	21	0.5
	29	26	0.6

[a] PNA and PANB are *p*-nitroaniline and *p*-amino-*p*′-nitrobiphenyl, respectively.

It is worth noting that the hydrogen atoms (H82 and H52) involved in intramolecular C−H···O hydrogen bonds increase their electron population in the bulk, contrary to those involved in intermolecular interactions. This opposite behavior is discussed in detail in a companion paper[21] and is due to the occurrence of the former interactions also in the gas phase.

Dipole and induced dipole moment—comparison with other systems: the resulting dipole magnitude in the crystal is comparable to that of a zwitterion like the L-alanine [12.9(7) D from X-ray data and 12.3 from gas-phase RHF/6-31G** calculations],[74] or of a nonlinear optical material containing nitro -groups such as the 2-methyl-4-nitroaniline [25(8) D from X-ray data and 19.5 or 8.8 D from gas-phase RHF/D95 calculations with and without an applied electric field],[75] or of DL-histidine [17.2(17) D from X-ray data, using a *k*′ restricted multipole model and 19.9 D from PHF-621G** calculations].[24] More interesting, however, are the absolute $|\Delta\boldsymbol{\mu}|$ and the relative $|\Delta\boldsymbol{\mu}|/|\boldsymbol{\mu}_{molOG}|$ magnitudes of the induced dipole in DMACB, as compared to those found in other systems. Table 4 shows that both quantities (experiment: $|\Delta\boldsymbol{\mu}| = 9.1$ D, $|\Delta\boldsymbol{\mu}|/|\boldsymbol{\mu}_{molOG}| = 1.25$, using the OG HF/6-21G data for the gas-phase reference; theory: $|\Delta\boldsymbol{\mu}| = 5.5$ D, $|\Delta\boldsymbol{\mu}|/|\boldsymbol{\mu}_{molOG}| = 0.75$) are greater than those found for molecules such as *p*-nitroaniline (PNA),[24] urea,[27,29] formamide,[29,76] DL-histidine,[24] DL-proline,[24] imidazole,[22] and water (ice VIII),[28,29] which in their crystals are held together by the much stronger N−H···O or O−H···O hydrogen bonds. Only *p*-amino-*p*′-nitrobiphenyl (PANB),[24] which has a large separation between the group acting as H acceptor (NO_2)

(74) Destro, R.; Bianchi, R.; Morosi, G. *J. Phys. Chem.* **1989**, *93*, 4447.
(75) Howard, S. T.; Hursthouse, M. B.; Lehmann, C. W.; Mallinson, P. R.; Frampton, C. S. *J. Chem. Phys.* **1992**, *97*, 5616.
(76) Gatti, C. Unpublished.

and that acting as H-donor (NH_2), seems to show definitely larger relative and absolute magnitudes of the induced dipole moment.[77]

Induced molecular dipole and packing energy: the molecular dipole enhancement in the crystal has importance first in its own right because of the related rearrangements in the molecule electron distribution and second because of the increase it induces on the dipolar contributions to the packing energy. If we restrict our attention to the intracolumn interaction within an AA′ or a BB′ pair—which are both characterized by a head-to-tail arrangement of the molecular dipole moments—the corresponding dipole−dipole interaction energy is more than tripled as compared to the value one would obtain using unperturbed molecular charge distributions. In fact, if $|\Delta\boldsymbol{\mu}/\boldsymbol{\mu}|$ amounts to 0.75 and the induced dipole is parallel to $\boldsymbol{\mu}$, the ratio of the density unperturbed vs the density perturbed interaction energies would be equal to $1 + 2\Delta\mu/\mu + (\Delta\mu/\mu)^2 = 3.06$.

Conclusions

We have shown that a highly significant molecular dipole enhancement (over 75%) may occur upon crystallization, despite the lack of a strongly hydrogen bonded environment in the crystal. The weak C−H···O interactions in the DMACB crystal induce a molecular dipole increase that is comparable and in many cases even larger than that found in systems which are tied together by the stronger O−H··O and N−H···O hydrogen bonds.[22,78] It is worth noting that the DMACB crystal represents a very interesting system for analyzing the dipole enhancement due to the weak C−H···O interactions, since no other kind of stronger and thus successfully competing hydrogen bonds, is present.

In the present work a new important role of the C−H···O bonds has been highlighted, in addition to those already listed and termed as *functions* by Steiner.[2] This new *function* has been derived through an analysis of the crystalline electron densities ρ, rather than from structural, spectroscopic, or thermodynamical approaches as occurred for most of the other functions.

The large enhancement of the dipole moment induced by the formation of weak C−H···O bonds is unlikely to be exclusive of the DMACB system. On the contrary, it should be a behavior common to other systems linked by C−H···O bonds and having a large separation between the groups acting as H acceptor and those acting as H-donor. Several examples have been published in the literature[2] where, in isomorphous crystal structures, a N/O−H···O hydrogen bond in one structure is isofunctionally replaced by a C−H···O interaction in the other. It would be important to study systems where such a replacement takes place so as to assess how the dipole enhancement induced by C−H···O bond formation compares to that caused by N/O−H···O bond formation in the corresponding isomorphous crystal structures.

Acknowledgment. This research has been supported by the Italian MURST and CNR. We thank Mario Bandera for helping us in the preparation of the drawings.

JA010316M

(77) Data in Table 4 are not homogeneous as they were derived by using different model approaches. As a consequence the $|\Delta\boldsymbol{\mu}|$ and $|\Delta\boldsymbol{\mu}|/|\boldsymbol{\mu}_{\mathrm{molOG}}|$ magnitudes and ordering reported in the table are to be taken in a qualitative way only.

(78) Koritsanszky, T. S.; Coppens, P. *Chem. Rev.* **2001**, *101*, 1583−1627.